6.5 BRED VECTORS AND FORECAST ERROR IN THE NASA COUPLED GENERAL CIRCULATION MODEL

Shu-Chih Yang[1*], Eugenia Kalnay[1], Ming Cai[3], Michele Rienecker[4] and Joaquim Ballabrera[1]

[1] University of Maryland, College Park, MD
[2] Florida State University, Tallahassee, FL
[3] NASA/Goddard Space Flight Center, Greenbelt, MD

1 INTRODUCTION

For the seasonal to interannual prediction (SIP), the forecast skill is strongly influenced by the model's ability to describe the SST variations. Ensemble prediction systems should be designed to capture such SST uncertainties and the consequent variations. Therefore, the evolution of the ensemble perturbations should carry the coupled characteristics associated with low frequency variations since the climate system is dominated by the slow, ocean-atmosphere coupled processes (i.e. ENSO). Methods of generating ensemble perturbations for ENSO prediction aim to determine how to create the initial perturbations wisely in order to capture the growth of such slowly varying, coupled instability so that the perturbations project onto the seasonal-to-interannual related uncertainties.

The breeding technique (Toth and Kalnay 1993, 1997) has been applied in simple coupled models (Cai et al., 2003, Peña and Kalnay 2004, Yang, 2005), showing that slowly varying coupled instabilities can be identified in the coupled bred vector when choosing physically meaningful breeding parameters. The breeding experiments of NASA CGCM under perfect model scenario have demonstrated that bred vectors have coupled properties related to the background ENSO variations and may have potential impact on ENSO prediction (Yang et al. 2005). They also showed that the bred vectors obtained with the NASA and the NCEP coupled GCMs have very similar characteristics.

In the present study, we perform breeding experiments with a much more challenging system: the operational CGCM with real observations involved. As the first step to explore the applications in ensemble forecasting, we examine the relationship between bred vector, one-month forecast error and the background anomalies in a realistic system. We find that the bred vectors are strongly related to the monthly forecast errors, so that their relationship can be used in ocean data assimilation by providing the system with the flow-dependent "errors of the month".

2 Breeding in the NSIPP operational CGCM

The NSIPP coupled model is a fully coupled global ocean-atmosphere-land system developed at NASA Goddard Space Flight Center (GSFC) (http://nsipp.gsfc.nasa.gov). It is comprised of the NSIPP-atmospheric general circulation model (AGCM) the Poseidon Ocean model (OGCM), and the Mosaic land surface model. The initial state of the OGCM uses the analysis fields from the univariate optimal interpolation (OI) assimilation scheme. The AGCM is initialized with AMIP-style atmospheric states. The procedure of a breeding cycle is done as in Yang et al. (2005). The bred vector is the differences between the perturbed and unperturbed runs. In our experiments, the oceanic-bred perturbations are added to oceanic analysis fields, and atmospheric bred perturbations are added to AMIP restart fields. The bred perturbation is measured by the rms of the BV SST in the Niño3 region and rescaled to the magnitude of 0.085°C. Also, the rescaling period is chosen to be one month, which is important to capture the slow coupled instability. The experiments are performed from January 1993 to November 1998. The one-month forecast error is defined as the difference between the analysis field and its first month forecast.

3 RESULTS

3.1 Bred vector, one-month forecast error and background temperature anomalies

Our results indicate that bred vectors show a structure similar to the one-month forecast errors in many aspects. For example, both the forecast error and the bred vector (BV) growth rate are very sensitive to the ENSO phases (Niño3 index), showing low frequency variations, and their temporal evolutions agree with each other very well. Similarly, the SST forecast error is also very sensitive to the background ENSO phases and particularly small during strong El Niño. We analyze the relationship among BV, forecast error and background SST anomalies in a statistical sense. The result (Fig. 1) suggests that the pattern correlation between the bred vector and the forecast errors is particularly good when the bred vector growth rate is large; indicating that the dynamical processes dominate the one-month forecast error will also strongly influence the shapes of bred vectors. In addition, the subsurface temperature of bred vector and the one-month forecast error also show a strong sensitivity to the phase of an ENSO event as shown in Fig. 2. For the 1997 warm event, the forecast error appeared in the subsurface of the western Pacific at the early stages, then

* *Corresponding author address*: Shu-Chih Yang, Univ. of Maryland, Earth System Science Interdisciplinary Center, College Park, MD. 20742-2465. emai: scyang@atmos.umd.ed

propagated to the eastern Pacific and amplified. Bred vectors capture well where the large forecast error is located, including its dynamical eastward propagation. We applied EOF analysis to represent the dominant structures (Fig. 4 and Fig. 5) of the bred vector and forecast error and compared with the ENSO modes of the background subsurface temperature anomaly along the equator (Fig. 3). Our results show that the dominant structures in the bred vector and forecast error are very similar. The structure is large-scale and largely projects on the variability associated with the ENSO variability. We also found that such property remains even with different rescaling norms[**]. This is reasonable since the dynamic errors lie in an attractor whose dimensionality is much lower than the system dimension. As shown in Fig. 3, the first two EOF modes of background temperature variability, involved mainly with ENSO evolutions, already explain about 70% of the total variability. Therefore, this constrains the error structure in space. Based on the three set of BV SSTs with different rescaling norms, we calculate locally (~300km by 300km) how much they can explain the forecast error. We found that the local projection of the forecast error on the subspace spanned by three bred vectors is larger than the projection on the subspace spanned by three operational perturbations, which are represented by the differences between two randomly selected analysis states. The result is valid for both tropics and extra-tropics.

3.2 Implications for oceanic error structures in the tropical Pacific

The spatial correlation between the bred vector and forecast error suggests bred vectors can be used to identify the shapes of the fast growing instabilities that dominate the forecast error. Such implication can be quantified by examining the zonal and meridional error correlation lengths estimated from bred vector and forecast error. For this purpose, we first estimate the correlation lengths by fitting the error covariance of bred vector and forecast error with a Gaussian function. Note that in the OI scheme, a simple time-independent Gaussian function is used to update the analysis field (Troccoli and Haines, 1999). Our results suggest that for the meridional direction, the correlation scales estimated from forecast error and bred vector are similar to the value used in the OI (~400km). However, for the zonal direction, their correlation lengths near the equator are much shorter than the value used in the OI (~1500km). Generally, the zonal correlation length from monthly bred vector has similar trend compared to the forecast error and exhibits similar scales. The results of Gaussian fitting are summarized in Table 1. The last two columns (the fitted variance) reflect the fact that the largest variabilities take place near the equator, associated with the shallower (and more unstable) thermocline.

[**] We used three different rescaling norms to measure the growth of the perturbations: (1) SST norm in the Niño3 region and breeding globally, (2) the thermocline in the tropical Pacific and (3) the SST norm in the Nino3 region but breeding only in the tropics.

4. SUMMARY

In this study, we examined the characteristic and relationship between bred vector and the one-month forecast error in order to explore potential applications to use the bred vector as initial coupled ensemble perturbations for ensemble forecasting. Our results indicate that the one-month forecast error and the bred vectors share many common characteristics in the SST and subsurface temperature structure in both space and time. Our results indicate that the one-month forecast error in NSIPP CGCM is dominated by dynamical errors whose shape can be captured by bred vectors. Such agreement is especially good when the BV growth rate is large. At the peak of ENSO episodes the growth rate and error growth are low, in agreement with Cai et al (2003).

Our results suggest the potential impact from using the bred vector to represent the features of forecast error, such as initial ensemble perturbations for capturing the uncertainties related with seasonal-to-interannual variability. Due to the heavy computational cost of CGCM, the operational ensemble size is limited. Therefore, using bred perturbations should allow small ensembles to perform efficiently by projecting the perturbation evolution on the seasonal-to-interannual associated features.

In addition, the ability of bred vectors to detect the month to month forecast error variability should allow the oceanic data assimilation scheme with simple covariance having monthly flow-dependent variations in the SST and subsurface. Our preliminary results show that the mean correlation length estimated from bred vector and one-month forecast error have much shorter zonal scales than what has been prescribed in the OI scheme. If these shorter scales are used within the OI system, it may cause the analysis corrections to over-emphasize small scale structures. In stead, it is possible to use a hybrid background error covariance that combines the standard OI background error correlation with information on the “errors of the month” provided by the bred vectors. Experiments with a Quasi-Geostrophic model suggest that this approach can attain a level of accuracy comparable to 4D-Var, at a very low computational cost (Yang et al, 2005).

5. REFERENCES

Cai, E. Kalnay, and Z. Toth, 2003: Bred vectors of the Zebiak-Cane model and their application to ENSO predictions. *J. Climate*, **16**, 40-55.

Peña, M. and E. Kalnay, 2004: Separating fast and slow modes in coupled chaotic system. *Nonlinear Process. Geophys.*, **11**, 319-327.

Troccoli, A. and K. Haines, 1999: Use of the temperature–salinity relation in a data assimilation context. *J. Atmos. Oceanic. Tech.*, **16**, 2011–2025.

Toth, Z. and E. Kalnay, 1993: Ensemble forecasting at NMC: the generation of perturbations. *Bull. Amer. Meteor. Soc.*, **74**, 2317-2330.

___ and ___, 1997: Ensemble forecast at NCEP and the breeding Method. *Mon. Wea. Rev.*, **125,** 3297-3319.

Yang, S-C, M. Cai, E. Kalnay, M. Rienecker, G. Yuan and Z. Toth: ENSO Bred Vectors in Coupled Ocean-Atmosphere General Circulation Models. *J. Climate,* in press.

------, 2005: Bred Vectors In The NASA NSIPP Global Coupled Model and Their Application To Coupled Ensemble Predictions And Data Assimilation. PhD thesis.. University of Maryland, 174 pages. Available at http://www.atmos.umd.edu/ ~ekalnay

------, M. Corazza, A. Carrassi, E. Kalnay, and T. Miyoshi, 2005: Comparison of ensemble-based and variational-based data assimilation schemes in a quasi-geostrophic model. Extended abstract for AMS Symposium on Observations, Data Assimilation and Probabilistic Prediction, Atlanta, Georgia, 2006.

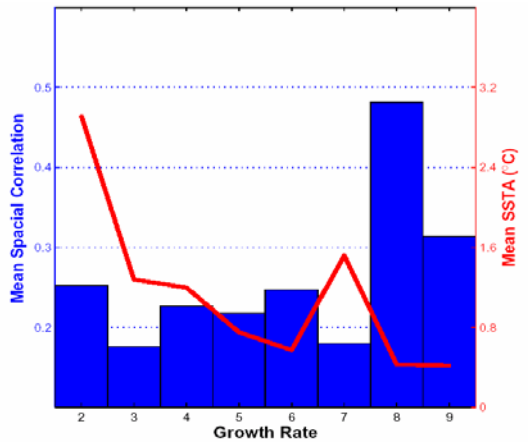

Fig. 1: Mean value of the pattern correlation (bar) and the Niño3 index (red line) in bins defined by the BV growth rate. Pattern correlations and the Niño 3 index are also grouped based on their corresponding growth rate. Pattern correlation is defined as the absolute value of the spatial correlation between the bred vector and analysis increment in the Niño3 region. The figure shows that large SSTA are associated with low BV growth rate (i.e., that errors don't grow much at the peak of the ENSO episodes), and that large correlations between bred vectors and forecast errors occur when there is large BV growth rate.

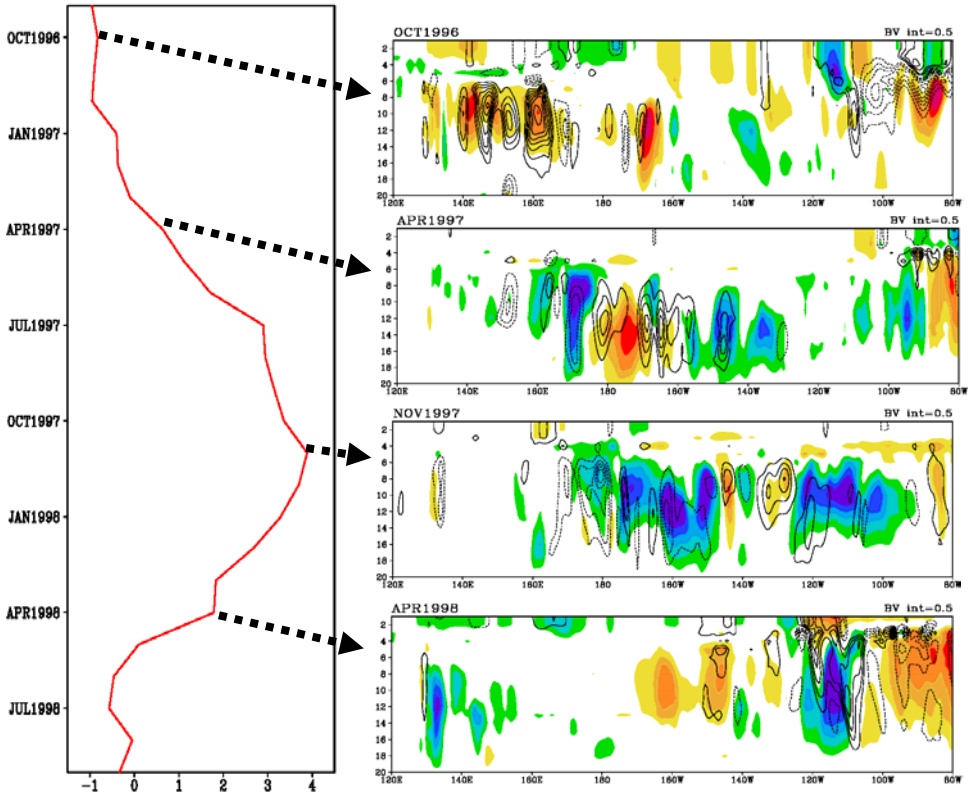

Fig. 2: (a) Background Niño3 index (°C) and vertical cross-section of temperature analysis increment (°C, color) and BV temperature (°C , contour) corresponding to (a) October 1996, before warming developed (b) April 1997, warming started (c) November 1997, warming is strongest, and (d) April 1998, warming diminished. Contours are plotted only when |BV temperature| is larger than 0.5 °C. This figure shows that the BV and the one-month forecast error (analysis increment) are strongly related.

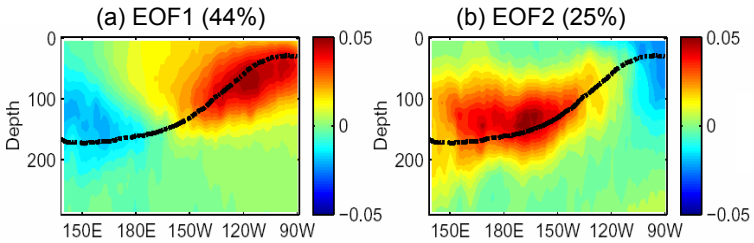

Fig. 3 First two EOF modes of the equatorial temperature anomaly representing 44% and 25% of the variance. The thick dashed line is the depth of the mean thermocline. EOF modes are normalized.

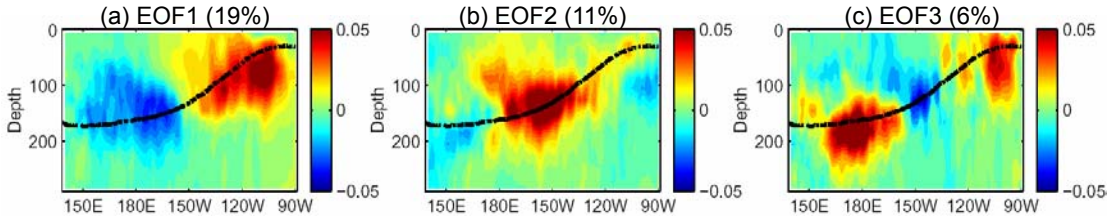

Fig. 4 First three EOF modes of equatorial temperature of analysis increment.

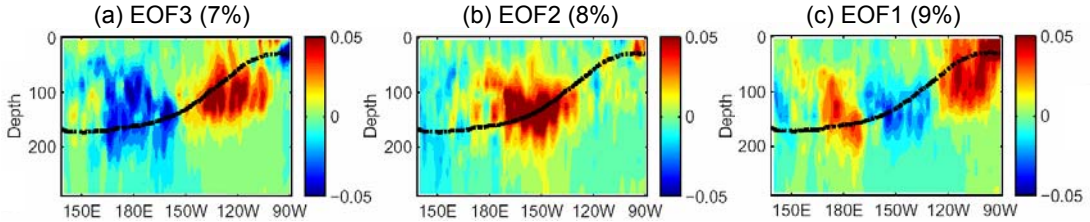

Fig. 5 First three EOF modes of equatorial temperature of the unrescaled bred vector, in reverse order.

Table 1 The error zonal correlation lengths and mean error variance of SST, obtained by fitting the bred vector and forecast error with a Gaussian function $f(r) = C_0 \exp[-\frac{r^2}{L^2}]$ The operational OI system assumes a zonal error correlation length of about 1500 Km.

Latitude	***L* (Km)**		**STD of *L* (Km)**		***C*₀**	
	forecast error	bred vector	Forecast error	bred vector	forecast error	bred vector
2.5°~7.5°	514	540	272	269	0.63	0.05
-2.5°~2.5°	575	505	251	226	0.99	0.14
-7.5°~-2.5°	445	416	217	199	0.83	0.07